IOP PUBLISHING CLASSICAL AND QUANTUM GRAVITY

Class. Quantum Grav. **25** (2008) 065005 (17pp) doi:10.1088/0264-9381/25/6/065005

Sensitivity and parameter-estimation precision for alternate LISA configurations

Michele Vallisneri, Jeff Crowder and Massimo Tinto

Jet Propulsion Laboratory, California Institute of Technology, Pasadena, CA 91109, USA

E-mail: Michele.Vallisneri@jpl.nasa.gov

Received 24 October 2007, in final form 4 February 2008
Published 4 March 2008
Online at stacks.iop.org/CQG/25/065005

Abstract

We describe a simple framework to assess the LISA scientific performance (more specifically, its sensitivity and expected parameter-estimation precision for prescribed gravitational-wave signals) under the assumption of failure of one or two inter-spacecraft laser measurements (*links*) and of one to four intra-spacecraft laser measurements. We apply the framework to the simple case of measuring the LISA sensitivity to monochromatic circular binaries, and the LISA parameter-estimation precision for the gravitational-wave polarization angle of these systems. Compared to the six-link baseline configuration, the five-link case is characterized by a small loss in signal-to-noise ratio (SNR) in the high-frequency section of the LISA band; the four-link case shows a reduction by a factor of $\sqrt{2}$ at low frequencies, and by up to ~ 2 at high frequencies. The uncertainty in the estimate of polarization, as computed in the Fisher-matrix formalism, also worsens when moving from six to five, and then to four links: this can be explained by the reduced SNR available in those configurations (except for observations shorter than three months, where five and six links do better than four even with the same SNR). In addition, we prove (for generic signals) that the SNR and Fisher matrix are invariant with respect to the choice of a basis of TDI observables; rather, they depend only on which inter-spacecraft and intra-spacecraft measurements are available.

PACS numbers: 04.80.Nn, 95.55.Ym

(Some figures in this article are in colour only in the electronic version)

1. Introduction

LISA (the Laser Interferometer Space Antenna) is a deep-space mission planned jointly by the National Aeronautics and Space Administration and the European Space Agency. LISA seeks to detect and study gravitational waves (GWs) in the mHz frequency band. It consists of three spacecraft flying in a triangular formation, whose relative positions will be monitored

by way of laser interferometry [1]. In contrast to ground-based interferometric GW detectors, LISA will have multiple readouts, for the six laser links between the spacecraft (one in each direction across each arm). These data streams, properly time shifted and linearly combined, provide observables that are insensitive to laser-frequency fluctuations and optical-bench motions, and that have different couplings to GWs and to the remaining system noises [2]. This technique is known as time-delay interferometry (TDI). Early on it was realized that different TDI observables can be built from different subsets of the six inter-spacecraft laser measurements [3], thus providing failure resistance against the loss of one or more measurements; furthermore, two or three linearly independent TDI observables can be used together to increase SNR and improve GW-parameter determination (this insight goes back at least to [4]).

In this paper we pull together and complete the results scattered throughout the TDI literature (see references in [2]) to build a simple framework that can assess the multi-observable LISA science performance when all measurements are available, and in failure scenarios where up to two of the six LISA inter-spacecraft measurements and up to four of the six intra-spacecraft measurements are lost. (We do not analyse the case of three lost inter-spacecraft laser-links: in this scenario, LISA cannot make wide-band measurements of gravitational radiation, but narrow-band measurements are still possible at frequencies equal to integer multiples of the inverse round-trip light time between the two spacecraft that preserve bidirectional laser measurements [5].)

In section 2 we introduce our notation and our model of the LISA measurement; in section 3, we describe a simple linear-algebra procedure to obtain the TDI observables that can be constructed in each LISA configuration; in section 4, we prove that any choice of a basis of observables can be used to compute the SNR and Fisher matrix, which depend only on the available measurements; in section 5, we give explicit expressions for the noise-orthonormal bases that simplify these computations; in sections 6 and 7, we apply our framework to the problem of determining the six-link, five-link and four-link LISA sensitivity to sinusoidal signals and its precision (i.e., the expected statistical error due to instrument noise) in the determination of the polarization of monochromatic binaries, thus quantifying the heuristic statement that additional TDI observables help disentangle the GW polarization states.

2. The LISA noise response

We adopt the 'classic' conceptualization of the LISA measurement developed by Armstrong, Estabrook and Tinto (see especially [3]), whereby: (i) each LISA spacecraft contains two optical benches, each with a proof mass and a laser; (ii) the inter-spacecraft one-way Doppler measurement 'y' on each bench consists of the fractional frequency difference between the incoming laser (bounced off the local proof mass) and the local laser (unbounced); (iii) the intra-spacecraft measurement 'z' on the same bench consists of the fractional frequency difference between the local laser (unbounced) and the laser from the other bench on the spacecraft, transmitted via optical fibre (and bounced on the other bench's proof mass). The noise in each of the measurements is modelled as due to the frequency fluctuations of the six lasers, to the random displacements of the six proof masses and of the six optical benches, and (for the y's) to shot noise and other optical-path noise in the low-SNR inter-spacecraft laser links. The optical-fibre noise can be removed by using the z's only in differences of the z's on the same bench; and the optical-bench motions along the lasers' lines of sight can be absorbed into the laser frequency noises. Without loss of generality, we also assume that the central frequencies of the lasers are all the same, and that all the Doppler beat notes due to the relative motions of the spacecraft have been removed via heterodyne measurements [6, 7].

Using the notation of [8, 9], the y and z noise responses are given by

$$y_{slr}^{\text{noise}}(t) = \begin{cases} C_s^*(t - L_l(t)) - C_r(t) + y_{slr}^{\text{op}}(t) - 2pm_r(t) & \text{for unprimed } l, \\ C_s(t - L_l(t)) - C_r^*(t) + y_{slr}^{\text{op}}(t) - 2pm_r^*(t) & \text{for primed } l, \end{cases} \tag{1}$$

and

$$z_{slr}^{\text{noise}}(t) = \begin{cases} C_r^*(t) - C_r(t) + 2pm_r^*(t) & \text{for unprimed } l, \\ C_r(t) - C_r^*(t) + 2pm_r(t) & \text{for primed } l, \end{cases} \tag{2}$$

where y_{slr} denotes the inter-spacecraft measurement obtained for the laser incoming from spacecraft s to spacecraft r, and travelling along link l (see figure 1; each link l sits across from spacecraft l in the LISA triangle, and takes a prime if slr is an odd permutation of 123); furthermore, z_{slr} denotes the intra-spacecraft measurement on the same bench as y_{slr} (this traditional notation is somewhat unfortunate, since the indices s and l refer to distant spacecraft that have no role in the local measurement). In these equations, the C_s and C_s^* represent the six laser frequency noises, the pm_r and pm_r^* the six proof-mass velocity fluctuations along the lasers' lines of sight, the y_{slr}^{op} the six inter-spacecraft optical-path noises, and L_l is the one-way light time along link l (the asterisks over the C and pm do not denote complex conjugation, but rather different noise variables).

TDI observables are linear combinations of several y and z, appropriately time delayed so that all instances of laser frequency noise (C_r and C_r^*) cancel out. It is useful to introduce time-delay operators $\mathcal{D}_l$ such that for any measurement $x(t)$,

$$\mathcal{D}_l x(t) \equiv x(t - L_l(t)), \quad \mathcal{D}_m \mathcal{D}_l x(t) \equiv x(t - L_l(t) - L_m(t - L_l(t))), \quad \ldots \tag{3}$$

and so on, with the shorthand $x_{;l}(t) \equiv \mathcal{D}_l x(t)$, $x_{;ml}(t) \equiv \mathcal{D}_m \mathcal{D}_l x(t)$, and so on. The time-delay operators commute only if the L_l are not functions of time, in which case the delays are usually denoted by subscripts set off by commas. For simplicity, in this paper we shall concern ourselves only with this case, which corresponds to 'modified' TDI observables. ('Second-generation' TDI observables are necessary to remove laser noise completely because of the 'breathing' of the LISA arms [10, 11]; however, when compared to the corresponding first-generation TDI observables, they engender only negligible corrections to the GW and secondary-noise responses, which are the building blocks of the SNR and Fisher matrix. Moreover, the second-generation observables can be approximated as finite-difference derivatives of their first-generation versions [9, 11], and this effect factors out in the computation of the SNR and Fisher matrix. For these reasons, the results of this paper remain valid for second-generation TDI.)

The problem of finding combinations of the y's and z's that cancel the six laser noises, C_s and C_s^*, can be reduced [11] to the problem of finding combinations of the new variables[1]

$$y'_{slr} = y_{slr} + \tfrac{1}{2}(z_{rl's,l} - z_{slr}), \tag{4}$$

which cancel the three equivalent laser noises $C'_s \equiv (C_s + C_s^*)/2$. This reduction removes the z's from consideration[2], and leads to the noise responses

[1] These substitutions are essentially equivalent, yet slightly different from those introduced in [11], with the advantage of leading to more symmetric noise responses.

[2] It would seem that working with the y' it becomes hard to enforce the constraint that the z be used only in the same-spacecraft differences $z_{231} - z_{32'1}$, $z_{312} - z_{13'2}$, $z_{123} - z_{21'3}$ (on spacecraft 1, 2 and 3 respectively), but this happens naturally in TDI combinations because of the way that the laser noises enter the y' noise responses. This is easy to see from the viewpoint of geometric TDI [9], where y' arrows that begin or end at the same spacecraft always appear in the sequences  (which involve the z difference at the spacecraft) or  (which involves neither of the z's at the spacecraft).

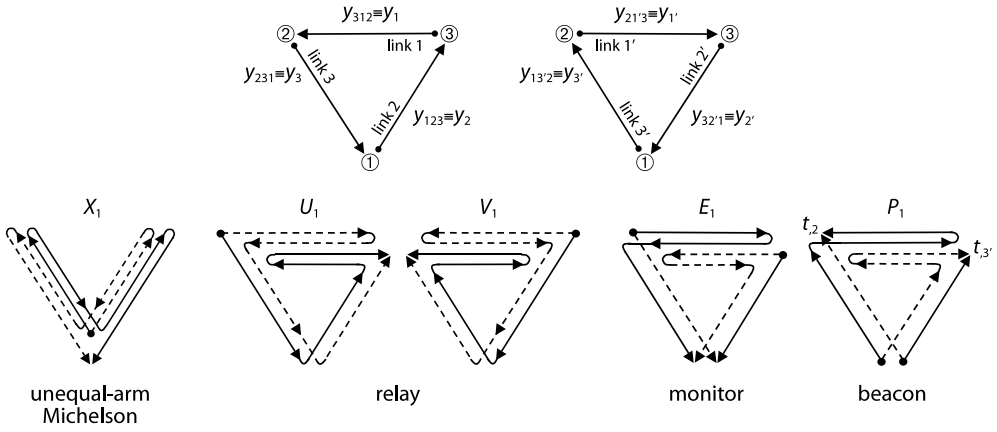

Figure 1. Top panel: the LISA inter-spacecraft measurements. Each arrow represents the frequency-comparison measurement $y_l \equiv y_{slr}$ taken on the spacecraft at the tip of the arrow between the incoming laser (moving in the direction of the arrow and experiencing the light time L_l) and the local laser. Unprimed (primed) link indices correspond to counter-clockwise (clockwise) laser propagation. Bottom panel: first-generation TDI observables as synthesized interferometers [9]. The four kinds of four-link observables are distinguished by the direction of the links converging on one spacecraft (in this case 1), which makes it a 'centre', 'relay', 'monitor' or 'beacon'.

$$y'^{\text{noise}}_{slr}(t) = \begin{cases} C'_{s,l} - C'_r + y^{\text{op}}_{slr} - 2pm_r + pm_{s,l} - pm^*_r & \text{for unprimed } l, \\ C'_{s,l} - C'_r + y^{\text{op}}_{slr} - 2pm^*_r + pm^*_{s,l} - pm_r & \text{for primed } l. \end{cases} \tag{5}$$

For terseness, in the rest of this paper we shall contract each of the index triples $312, 123, 231, 21'3, 32'1$ and $13'2$ to its middle link index alone, as shown at the top of figure 1, so that $y_l \equiv y_{slr}$ and $z_l \equiv z_{slr}$.

The recently proposed [12] LISA architecture with a single proof mass on each spacecraft and with 'strap-down' measurements (whereby the lasers are not bounced on the proof masses, but additional measurements are taken of the position of the latter with respect to the optical benches) would lead to analogous, but different noise responses. We expect the results of this paper to persist in the new architectures with slight modifications of (4), but careful verification is certainly indicated once the LISA architecture is finalized.

3. TDI observables from linear algebra and the LISA failure modes

When the delay operators commute, they have an especially useful representation in the Fourier domain,

$$\mathcal{D}_l\tilde{x}(f) = \Delta_l\tilde{x}(f), \qquad \mathcal{D}_m\mathcal{D}_l\tilde{x}(f) = \Delta_m\Delta_l\tilde{x}(f), \quad \ldots \tag{6}$$

where $\Delta_l = \exp 2\pi \mathrm{i} f L_l$. This representation turns the search for laser-noise-cancelling combinations into a problem of linear algebra. The laser-noise content of the y'_l measurements is described by the equation

$$\tilde{\mathbf{y}}' = D_6\tilde{\mathbf{C}}', \tag{7}$$

where $\tilde{\mathbf{y}}'$ is the vector $[y'_1, y'_2, y'_3, y'_{1'}, y'_{2'}, y'_{3'}]^T$, $\tilde{\mathbf{C}}' \equiv [C'_1, C'_2, C'_3]^T$, and

$$D_6 = \begin{pmatrix} 0 & -1 & \Delta_1 \\ \Delta_2 & 0 & -1 \\ -1 & \Delta_3 & 0 \\ 0 & \Delta_{1'} & -1 \\ -1 & 0 & \Delta_{2'} \\ \Delta_{3'} & -1 & 0 \end{pmatrix}; \tag{8}$$

now, a generic observable (not necessarily laser-noise-cancelling) is a linear combination $\mathbf{a}^T\tilde{\mathbf{y}}'$ (where '^{T}' denotes vector transposition), where the coefficients $\mathbf{a}$ will normally be polynomials of the Δ_l with integer coefficients. It follows from (7) that the $\mathbf{a}$ that correspond to laser-noise-cancelling observables must span the null space of D_6^T,

$$\mathbf{a}^T D_6 \tilde{\mathbf{C}}' = 0 \quad \Rightarrow \quad D_6^T \mathbf{a} = 0; \tag{9}$$

thus, the task of finding TDI observables reduces to finding a basis for null$\left(D_6^T\right)$, and *all* TDI observables can then be represented as linear combinations of the elements of that basis (although such representations may involve Δ_l's, and therefore delays, as we shall see in section 5.2). The Fourier-domain representation is especially suited to our goals of assessing the reduction in SNR associated with particular failure configurations, and of evaluating the parameter-estimation precision for observed gravitational signals, since these operations involve calculations performed in the Fourier domain.

The loss of one or more inter-spacecraft measurements results in the loss of the corresponding y'_l. However, the linear-algebra problem of (7) can still be formulated after removing the appropriate rows in $\tilde{\mathbf{y}}'$ and D_6. In general, if n is the number of measurements and m the number of laser noises to be cancelled, and if the subsetted D has full rank (which is generally the case), it follows that the dimension of null(D^T) is $r = n - m$. Thus, for 'full LISA', with six inter-spacecraft measurements and three noises, we can construct three independent TDI observables[3]; these are reduced to two after one measurement is lost, and to one after two are lost. In section 5 we describe which of the standard TDI observables can be reconstructed in each case.

The effects of losing one or more intra-spacecraft measurements are subtler. Consider for instance losing $z_{231} \equiv z_3$ (on spacecraft 1): from (4), we see that we immediately lose y'_3 and $y'_{3'}$; we also lose the ability of using y'_2 and $y'_{2'}$, which involve the other measurement on spacecraft 1, $z_{32'1} \equiv z_{2'}$ (remember that z_3 and $z_{2'}$ can appear only in the combination $z_3 - z_{2'}$ if fibre noise must be cancelled; thus, losing one or two z measurements on the same spacecraft is equivalent). However, it turns out that the combinations $y'_{3'} + y'_{3,3'}$ and $y'_2 + y'_{2',2}$ (in the graphic notation of geometric TDI [9], ⧹ and ⫽) contain neither z_3 nor $z_{2'}$ (and also no C'_1!). Thus we have four available measurements and two noises to be cancelled, so two independent TDI observables can be constructed. If some or all z measurements are lost on *two* spacecraft (say, 2 and 3) then only two combined measurements are available (in this case, $y'_3 + y'_{3',3}$ and $y'_{2'} + y'_{2,2'}$) with one laser noise to cancel, so a single independent TDI observable can be constructed (it is the unequal-arm Michelson centred on the non-faulty spacecraft). Last, if both inter- and intra-spacecraft measurements are lost, then at most one TDI observable can be constructed (and it is always an unequal-arm Michelson), and in some cases none. Again, see section 5. It is also possible to come to the same conclusions by working with a larger linear system that involves the available y_l (not y'_l), z_l and the six laser noises C_r and C_r^*.

[3] Although a combination of the three is insensitive to GWs in the long-wavelength limit because of symmetry; see figure 2.

4. Invariance of SNR and Fisher matrix by change of TDI basis

Of course, the basis of null(D^T) (with D the appropriate row-reduced matrix for the available measurements) is not unique; however, we now show that the total SNR and Fisher matrix are invariant with respect to the choice of a TDI basis, so *they depend only on which y_l and z_l measurements are available*, and they can be computed over any convenient basis. From the SVD decomposition [13]

$$\underbrace{D^T}_{m\times n} = \underbrace{U}_{m\times m} \cdot \underbrace{\Sigma}_{m\times n} \cdot \underbrace{V^\dagger}_{n\times n} \quad (\text{with } \Sigma_{ij} = 0 \text{ for } i \neq j), \tag{10}$$

it follows that a basis for null(D^T) is given by the columns of V that correspond to the 'extra' r null columns of Σ. The SVD decomposition is degenerate with respect to nonsingular linear combinations of these columns (i.e., with respect to choosing a different TDI basis). Calling W the $n \times r$ matrix of these columns, the optimal matched-filtering SNR for a source $\mathbf{h}(f)$ whose components are given by the individual TDI observables $X_\alpha = y'_i(t)W_{i\alpha}$ is given by

$$\begin{aligned}\mathrm{SNR}^2 &= 4\,\mathrm{Re}\int_0^{+\infty} h^\dagger_\alpha(f) S^{-1}_{\alpha\beta}(f) h_\beta(f)\,\mathrm{d}f \\ &= 4\,\mathrm{Re}\int_0^{+\infty} \mathbf{h}^\dagger(f)[W^T C(f) W^*]^{-1}\mathbf{h}(f)\,\mathrm{d}f,\end{aligned} \tag{11}$$

since

$$\begin{aligned}\tfrac{1}{2}S_{\alpha\beta}(f)\delta(f-f') &= \langle [y'_i(f)W_{i\alpha}][y'_j(f')W_{j\beta}]^*\rangle = W_{i\alpha}\langle y'_i(f) y'^*_j(f')\rangle W^*_{j\beta} \\ &= \tfrac{1}{2}W^T C(f) W^* \delta(f-f'),\end{aligned} \tag{12}$$

where the C_{ij} components are the secondary-noise cross-spectra of the individual y'_i. As discussed in appendix A, the matrix C_{ij} is in general complex and Hermitian.

If we change the TDI basis by means of a nonsingular linear transformation $\mathbf{h} \to B\mathbf{h}$ (so that we are computing $S_{\alpha'\beta'}$ over the TDI observables $X'_{\alpha'} = B_{\alpha'\alpha}X_\alpha = B_{\alpha'\alpha}y'_i(t)W_{i\alpha}$) we get

$$\begin{aligned}\mathbf{h}^\dagger[W^T C W^*]^{-1}\mathbf{h} \to \mathbf{h}^\dagger B^\dagger [B W^T C W^* B^\dagger]^{-1} B\mathbf{h} &= \mathbf{h}^\dagger B^\dagger (B^\dagger)^{-1}[W^T C W^*]^{-1} B^{-1} B\mathbf{h} \\ &= \mathbf{h}^\dagger [W^T C W^*]^{-1}\mathbf{h},\end{aligned} \tag{13}$$

so the SNR is invariant. Indeed, any noise inner product $(\mathbf{h}, \mathbf{g})$, and therefore the Fisher matrix elements $(\mathbf{h}_{,\mu}, \mathbf{h}_{,\nu})$, are also invariant under similar transformations.

As a corollary we get the intuitive fact that computing the SNR with an extra TDI observable that is a linear combination of the r others (which amounts to a $(r+1)\times r$ matrix B) does not change the result. To see this, we inject an additional $(r+1)\times(r+1)$ linear transformation B' that makes one of the $(r+1)$ TDI observables identically null; the entire product (13) can then be rewritten by dropping one of the rows of $B'B$, so we are back to the case of a nonsingular $r \times r$ transformation.

The equivalence of different TDI bases for the purpose of computing the Fisher matrix can also be proved with a different approach, closer to the reasoning of Romano and Woan [14]: we consider the estimation problem of determining the GW parameters *and* the laser frequency noises in the presence of secondary instrument noise, assumed Gaussian and stationary. The likelihood of the LISA data is then written in terms of the y'_i and their secondary-noise cross-spectra, and (without loss of generality) rewritten in a TDI/non-TDI basis where the first m components span null(D^T) and the other r span null(D^T)$^\perp$. We compute the Fisher matrix by taking derivatives of the log likelihood with respect to the GW parameters and to the individual frequency components of laser noise (again, our premise is that we are estimating these in addition to the GW parameters, even if in practice it will turn out that only some

combinations of the laser noises can truly be estimated from the LISA measurements). Using the Frobenius–Schur formula [15], we can then show that the GW-parameter sector of the inverse Fisher matrix (i.e., the expected covariance matrix for the GW-parameter estimators) is equal to the inverse of the TDI sector of the full Fisher matrix, with all the laser-noise components dropping out. Since the projection on the null(D^T) and null$(D^T)^\perp$ subspaces can be cast as a geometrical operation, we see that the Fisher matrix does not depend on the choice of TDI observables, but only on the geometry of null(D^T).

5. Noise-orthogonal bases of TDI observables

An especially useful linear transformation of a TDI basis is the one that leads to an orthonormal basis of $S_{\alpha\beta}$, since the SNR then has the simplified form

$$\mathrm{SNR}^2 = \sum_{\alpha'} 4\,\mathrm{Re} \int_0^{+\infty} \frac{{h_{\alpha'}}^\dagger(f) h_{\alpha'}(f)}{S_{\alpha'\alpha'}(f)}\,\mathrm{d}f; \tag{14}$$

a similar expression follows for the Fisher-matrix elements. We shall now work out such bases and the corresponding $S_{\alpha'\beta'}$ under various LISA failure modes.

5.1. Four-link configurations

We begin with the case of two lost y_l measurements, where null(D^T) has dimension one, so that essentially only one TDI observable can be constructed, which is trivially a noise-orthonormal basis. Depending on which measurements are lost, this observable is one of the standard four-link observables (unequal-arm-Michelson, relay, beacon and monitor) described in [11], and shown pictorially in the bottom part of figure 1. In this section we spell them out and identify them with a new compact naming scheme.

If the missing y_l are along the same arm (say, y_1 and y'_1), we can build the unequal-arm Michelson observable centred on spacecraft 1,

$$X_1 \equiv y'_{2'} + y'_{2,2'} + y'_{3,22'} + y'_{3',322'} - (y'_3 + y'_{3',3} + y'_{2',3'3} + y'_{2,2'3'3}); \tag{15}$$

the analogous X_2 and X_3 are obtained by the cyclic permutations $1 \to 2 \to 3$ and $1' \to 2' \to 3'$ (which will go without saying for all observables to follow). Note that these X_1, X_2 and X_3 are usually called X, Y and Z in the TDI literature, but here we prefer a notation that emphasizes which y_l enter them.

If the missing y_l are consecutive and 'codirected' (say, $y_{2'}$ and $y_{3'}$), we can build the 'forward' *relay* observable U_1 that goes through spacecraft 1 by way of links 3 and 2,

$$U_1 \equiv y'_{1'} + y'_{1,1'} + y'_{2,11'} + y'_{3,21'1} - (y'_2 + y'_{3,2} + y'_{1,32} + y'_{1',132}); \tag{16}$$

by contrast, the 'backward' relay observable V_1 goes through spacecraft 1 by way of $2'$ and $3'$,

$$V_1 \equiv y'_1 + y'_{1',1} + y'_{3',1'1} + y'_{2',1'13'} - (y'_{3'} + y'_{2',3'} + y'_{1',2'3'} + y'_{1,1'2'3'}). \tag{17}$$

If the missing y_l are consecutive, but have opposite 'directions', we have two cases. If the available measurements are (say) y_1 and $y_{1'}$, and also $y_{2'}$ and y_3 (which 'point' towards spacecraft 1), we can build the *monitor* observable

$$E_1 \equiv y'_3 + y'_{1,3} + y'_{1',31} - y'_{2'} - y'_{1',2'} - y'_{1,2'1'} + y'_{2',1'1} - y'_{3,1'1}; \tag{18}$$

whereas if the available measurements other than y_1 and $y_{1'}$ are y_2 and $y_{3'}$ (which 'point' away from spacecraft 1), we can build the *beacon* observable

$$P_1 \equiv y'_{1,2} + y'_{1',21} + y'_{3',211'} - y'_{1',3'} - y'_{1,3'1'} - y'_{2,3'1'1} + y'_{2,3'} - y'_{3',2}. \tag{19}$$

Table 1. Standard TDI observables available in various LISA failure modes. For a single lost y_l, all TDI observables on the corresponding line (or column) of the left table are available (and any two of them are independent); for two lost y_l, only the observable at the corresponding intersection is available. For one or two lost z_l on the same spacecraft, the two TDI observables on the corresponding line (or column) of the right table are available; for two to four lost z_l on two spacecraft, only the observable at the intersection is available. For mixed failure modes, at most one X_l observable is available, as can be seen by intersecting the two tables.

	y_1	y_2	y_3	$y_{1'}$	$y_{2'}$	$y_{3'}$
y_1		V_3	V_2	X_1	E_3	P_2
y_2	V_3		V_1	P_3	X_2	E_1
y_3	V_2	V_1		E_2	P_1	X_3
$y_{1'}$	X_1	P_3	E_2		U_3	U_2
$y_{2'}$	E_3	X_2	P_1	U_3		U_1
$y_{3'}$	P_2	E_1	X_3	U_2	U_1	

	z_l on 1	z_l on 2	z_l on 3
z_l on 1		X_3	X_2
z_l on 2	X_3		X_1
z_l on 3	X_2	X_1	

Again, the analogous observables E_2, E_3, P_2 and P_3 can be obtained by cyclic permutations. The left part of table 1 shows which observable is available in each case: look at the intersection of the row and column corresponding to the missing y_l.

We can now compute the noise PSDs for these observables by writing them in the Fourier domain in terms of the $\tilde{y}_l$ and of the complex Δ_l, multiplying them by their complex conjugates, and substituting the noise responses (5). We work in the limit of equal armlengths (so all $\Delta_l = \exp 2\pi \mathrm{i} f L$) and assume that all noises are Gaussian and uncorrelated (i.e., have null cross-spectra), and have spectral densities $S^{\mathrm{op}}(f)$ for the optical-path noises and $S^{\mathrm{pm}}(f)$ for the proof-mass noises[4]. The resulting PSDs are

$$S_{X_l}(f) = 16\, S^{\mathrm{op}} \sin^2 x + 16\, S^{\mathrm{pm}}[3 + \cos 2x] \sin^2 x, \tag{20a}$$

$$S_{U_l}(f) = S_{V_l}(f) = 8\, S^{\mathrm{op}}[4 + 4\cos x + \cos 2x] \sin^2 \frac{x}{2} + 16\, S^{\mathrm{pm}}[5 + 5\cos x + 2\cos 2x] \sin^2 \frac{x}{2}, \tag{20b}$$

$$S_{E_l}(f) = S_{P_l}(f) = 8\, S^{\mathrm{op}}[3 + 2\cos x] \sin^2 \frac{x}{2} + 16\, S^{\mathrm{pm}}[3 + \cos x] \sin^2 \frac{x}{2}, \tag{20c}$$

where $x = 2\pi f L$.

5.2. *Five-link configurations*

If one y_l is lost, $\mathrm{null}(D^T)$ has dimension two, corresponding to two independent TDI observables. Depending on which y_l is missing, a different set of the five standard observables described in the last section can be constructed, as given by the rows of the left part of table 1. Within each set, any two observables can form a basis for $\mathrm{null}(D^T)$. This means also that any two observables can be used to re-express any other. To find such relations, we solve linear systems such as

$$X_1 = c(X_1, V_2) V_2 + c(X_1, V_3) V_3, \tag{21}$$

[4] For reference, the standard LISA model used in the Mock LISA Data Challenges [16] has $(S^{\mathrm{op}})^{1/2} = 20 \times 10^{-12}\,\mathrm{m\,Hz^{-1/2}}$, $(S^{\mathrm{pm}})^{1/2} = 3 \times 10^{-15}[1 + (10^{-4}\,\mathrm{Hz}/f)^2]^{1/2}\,\mathrm{m\,s^{-2}\,Hz^{-1/2}}$ and $L = 16.6782$ s.

and therefore

$$\begin{pmatrix} 0 \\ 0 \\ \Delta_{2'} - \Delta_{2'}\Delta_{3'}\Delta_3 \\ 1 - \Delta_{3'}\Delta_3 \\ -1 + \Delta_2\Delta_{2'} \\ -\Delta_3 + \Delta_3\Delta_2\Delta_{2'} \end{pmatrix} = \begin{pmatrix} 0 & 0 \\ -1 + \Delta_{2'}\Delta_2 & -\Delta_{2'} + \Delta_{2'}\Delta_{3'}\Delta_3 \\ 1 - \Delta_{2'}\Delta_{3'}\Delta_{1'} & 0 \\ -\Delta_{3'}\Delta_{1'} + \Delta_2 & -1 + \Delta_{3'}\Delta_3 \\ 0 & 1 - \Delta_{1'}\Delta_{2'}\Delta_{3'} \\ -\Delta_{1'} + \Delta_{1'}\Delta_{2'}\Delta_2 & -\Delta_{1'}\Delta_{2'} + \Delta_3 \end{pmatrix} \begin{pmatrix} c(X_1, V_2) \\ c(X_1, V_3) \end{pmatrix}, \tag{22}$$

which yields

$$X_1 = \frac{\Delta_{2'} - \Delta_{2'}\Delta_{3'}\Delta_3}{1 - \Delta_{3'}\Delta_{1'}\Delta_{2'}} V_2 + \frac{\Delta_2\Delta_{2'} - 1}{1 - \Delta_{3'}\Delta_{1'}\Delta_{2'}} V_3 \tag{23}$$

and finally

$$X_1 - X_{1,3'1'2'} = V_{2,2'} - V_{2,2'3'3} + V_{3,22'} - V_3. \tag{24}$$

Analogously,

$$X_{1,132} - X_1 = U_{2,3'3} - U_2 + U_{3,3} - U_{3,322'}, \tag{25a}$$

$$X_{1,32} - X_{1,1'} = P_2 - P_{2,3'3} + E_{3,322'} - E_{3,3}, \tag{25b}$$

$$X_{1,3'2'} - X_{1,1} = E_{2,2'3'3} - E_{2,2'} + P_3 - P_{3,22'}, \tag{25c}$$

and also

$$V_{2,1'} - V_{2,32} = P_{2,3'1'} - P_{2,2} + E_{3,1'} - E_{3,1'2'2}, \tag{26a}$$

$$V_{3,1'} - V_{3,32} = P_2 - P_{2,3'3} + E_{3,1'2'} - E_{3,3}, \tag{26b}$$

$$U_{2,2'3'} - U_{2,1} = E_{2,31} - E_{2,2'} + P_3 - P_{3,22'}, \tag{26c}$$

$$U_{3,2'3'} - U_{3,1} = E_{2,1} - E_{2,133'} + P_{3,21} - P_{3,3'}. \tag{26d}$$

(Since these equations cease to hold strictly if the delays become noncommutative, here the ordering of the delay indices has little actual meaning.)

We now seek a basis of two noise-orthogonal TDI observables by diagonalizing the cross-spectrum matrix $S_{\alpha\beta}$ of two of the five standard observables, under the assumptions on the noises given above. The diagonalization process has different (but equally valid) results depending on which two we use, but not all choices are equally convenient. For instance, if y_1 is lost and we work with P_2 and E_3, we obtain a correlation matrix that has two equal terms on the diagonal (see (20*c*)) and *complex* cross terms

$$S_{P_2E_3} = S^*_{E_3P_2} = 4 \sin\frac{x}{2} \sin x \, \mathrm{e}^{\mathrm{i}x/2}[S^{\mathrm{op}}(3 + \mathrm{e}^{\mathrm{i}x}) + 2\,S^{\mathrm{pm}}(3 - \mathrm{e}^{-\mathrm{i}x})]. \tag{27}$$

Unfortunately, the resulting eigenvectors are $\propto E_3 - \mathrm{e}^{\mathrm{i}\phi(f)}P_2$ and $E_3 + \mathrm{e}^{\mathrm{i}\phi(f)}P_2$, with $\phi(f) = \arg(S_{P_2E_3})$; that is, they have complex and frequency-dependent coefficients, whereas we are used to orthogonal observables that are real variables and have integer coefficients. The same problem occurs if we diagonalize the cross-spectrum matrix for any two out of X_1, V_2, V_3, P_2, E_3. After some experimenting, we find that the linear combinations $P_2 - X_1/2$ and $E_3 + X_1/2$ do have a real cross-spectrum; diagonalizing them yields the eigenvectors

$$A^{(1)} = (P_2 - E_3 - X_1)/\sqrt{2}, \qquad E^{(1)} = (P_2 + E_3)/\sqrt{2}, \tag{28}$$

with PSDs

$$S_{A^{(1)}} = 8\,S^{\rm op}[2+\cos x]^2 \sin^2\frac{x}{2} + 8\,S^{\rm pm}[14+15\cos x+6\cos 2x+\cos 3x]\sin^2\frac{x}{2}, \tag{29a}$$

$$S_{E^{(1)}} = 8\,S^{\rm op}[2+\cos x]^2 \sin^2\frac{x}{2} + 32\,S^{\rm pm}[2+\cos x]^2 \sin^2\frac{x}{2}. \tag{29b}$$

Working through a similar exercise when $y_{1'}$ is lost yields

$$A^{(1')} = (P_3 - E_2 - X_1)/\sqrt{2}, \qquad E^{(1')} = (P_3 + E_2)/\sqrt{2}, \tag{30}$$

with the same PSDs. Once again, cyclic index permutations will yield orthonormal basis for the other missing y_l.

5.3. Full six-link configuration

Here null$\left(D_6^T\right)$ has dimension three, and all standard observables can be constructed. An obvious choice is to diagonalize the three unequal-arm Michelson observables, which have cross-spectra

$$S_{X_iX_j} = -8\,S^{\rm op}\cos x\sin^2 x - 32\,S^{\rm pm}\cos x\sin^2 x \qquad (i\neq j) \tag{31}$$

and yield the well-known eigenvectors

$$\begin{aligned} A^{(X)} &= (X_3 - X_1)/\sqrt{2}, \qquad E^{(X)} = (X_1 - 2X_2 + X_3)/\sqrt{6}, \\ T^{(X)} &= (X_1 + X_2 + X_3)/\sqrt{3}, \end{aligned} \tag{32}$$

with PSDs

$$S_{A^{(X)}} = S_{E^{(X)}} = 8\,S^{\rm op}[2+\cos x]\sin^2 x + 16\,S^{\rm pm}[3+2\cos x+\cos 2x]\sin^2 x, \tag{33a}$$

$$S_{T^{(X)}} = 16\,S^{\rm op}[1-\cos x]\sin^2 x + 128\,S^{\rm pm}\sin^2 x\sin^4\frac{x}{2}. \tag{33b}$$

Less well known is the fact that E_1, E_2 and E_3 and P_1, P_2 and P_3 are also suitable bases. Since

$$S_{P_iP_j} = S_{E_iE_j} = 4\,S^{\rm op}\sin^2 x - 8\,S^{\rm pm}[-1+2\cos x]\sin^2 x, \qquad (i\neq j), \tag{34}$$

the resulting eigenvectors have structure similar to (32),

$$\begin{aligned} A^{(E)} &= (E_3 - E_1)/\sqrt{2}, \qquad E^{(E)} = (E_1 - 2E_2 + E_3)/\sqrt{6}, \\ T^{(E)} &= (E_1 + E_2 + E_3)/\sqrt{3}, \end{aligned} \tag{35}$$

and

$$\begin{aligned} A^{(P)} &= (P_3 - P_1)/\sqrt{2}, \qquad E^{(P)} = (P_1 - 2P_2 + P_3)/\sqrt{6}, \\ T^{(P)} &= (P_1 + P_2 + P_3)/\sqrt{3}, \end{aligned} \tag{36}$$

with PSDs

$$S_{A^{(E,P)}} = S_{E^{(E,P)}} = 8\,S^{\rm op}[2+\cos x]\sin^2\frac{x}{2} + 16\,S^{\rm pm}[3+2\cos x+\cos 2x]\sin^2\frac{x}{2}, \tag{37a}$$

$$S_{T^{(E,P)}} = 8\,S^{\rm op}[5+4\cos x]\sin^2\frac{x}{2} + 32\,S^{\rm pm}[5+4\cos x]\sin^4\frac{x}{2}. \tag{37b}$$

By contrast, working with U_1, U_2 and U_3 (or V_1, V_2 and V_3) leads to complex cross-spectra (although rather symmetric, with $S_{U_1U_2} = S_{U_2U_3} = S_{U_3U_1} = S^*_{U_2U_1} = S^*_{U_3U_2} = S^*_{U_1U_3}$), and two

out of three of the resulting eigenvectors have complex coefficients, and do not correspond to real observables (the third eigenvectors are again the completely symmetric $(U_1+U_2+U_3)/\sqrt{3}$ and $(V_1+V_2+V_3)/\sqrt{3}$).

The classic noise-orthogonal observables are perhaps the A, E and T of [17, 18], written in terms of the first-generation–TDI Sagnac observables

$$\alpha = y'_{2'} + y'_{1',2'} + y'_{3',1'2'} - (y'_3 + y'_{1,3} + y'_{2,13}), \tag{38}$$

(with β and γ obtained by cyclical permutations), which are a basis for null(D^T) only if $\Delta_l = \Delta_{l'}$, and have PSDs

$$S_{\alpha\alpha} = S_{\beta\beta} = S_{\gamma\gamma} = 6\,S^{\mathrm{op}} + 8\,S^{\mathrm{pm}}[5 + 4\cos x + 2\cos 2x]\sin^2\frac{x}{2}, \tag{39a}$$

$$S_{\alpha\beta} = S_{\beta\gamma} = S_{\gamma\alpha} = 2\,S^{\mathrm{op}}[2\cos x + \cos 2x] + 4\,S^{\mathrm{pm}}[\cos x - 1], \tag{39b}$$

yielding the eigenvectors

$$\begin{aligned} &A = (\gamma - \alpha)/\sqrt{2}, \qquad E = (\alpha - 2\beta + \gamma)/\sqrt{6}, \\ &T = (\alpha + \beta + \gamma)/\sqrt{3} \end{aligned} \tag{40}$$

with PSDs

$$S_A = S_E = 8\,S^{\mathrm{op}}[2 + \cos x]\sin^2\frac{x}{2} + 16\,S^{\mathrm{pm}}[3 + 2\cos x + \cos 2x]\sin^2\frac{x}{2}, \tag{41a}$$

$$S_T = 2\,S^{\mathrm{op}}[1 + 2\cos x]^2 + 8\,S^{\mathrm{pm}}\sin^2\frac{3x}{2}. \tag{41b}$$

If $\Delta_l \neq \Delta_{l'}$ we need the more complicated

$$\begin{aligned} \alpha_1 = {} & y'_{2'} + y'_{1',2'} + y'_{3',1'2'} + y'_{3,3'1'2'} + y'_{1,33'1'2'} + y'_{2,133'1'2'} \\ & - (y'_3 + y'_{1,3} + y'_{2,13} + y'_{2',213} + y'_{1',2'213} + y'_{3',1'2'213}) \end{aligned} \tag{42}$$

(and similarly for α_2 and α_3), which again have (32)-like eigenvectors $\bar{A}$, $\bar{E}$ and $\bar{T}$, and PSDs

$$S_{\bar{A}} = 4\sin^2\frac{3x}{2} \times S_A, \qquad S_{\bar{E}} = 4\sin^2\frac{3x}{2} \times S_E, \tag{43}$$

since in the limit $\Delta_l \to \Delta_{l'}$ $\alpha_1 \simeq \alpha - \alpha_{123}$, and so on.

5.4. Missing-z_l configurations

For lost z_l on two spacecraft we go back to the unequal-arm Michelson four-link scenario, as we do for certain combinations of lost y_l and z_l; the only scenario that remains to be covered is one of lost z_l on a single spacecraft (say, 1), where two unequal-arm Michelson observables (in this case, X_2 and X_3) can be constructed. From (20*a*) and (31) we get the eigenvectors

$$A^{(z1)} = (X_2 - X_3)/\sqrt{2}, \qquad E^{(z1)} = (X_2 + X_3)/\sqrt{2}, \tag{44}$$

and the PSDs

$$S_{A^{(z1)},E^{(z1)}} = 8\,S^{\mathrm{op}}[2 \pm \cos x]\sin^2 x + 8\,S^{\mathrm{pm}}[6 \pm 4\cos x + 2\cos 2x]\sin^2 x; \tag{45}$$

in the $\pm$ signs, the + refers to $A^{(z1)}$, the $-$ to $E^{(z1)}$.

6. The LISA sensitivity with four, five and six inter-spacecraft measurements

To illustrate the use of noise-orthogonal TDI bases, we now compute the sky-averaged LISA sensitivity to monochromatic, sinusoidal signals using four, five and six y_l measurements. We adopt the expressions of Vallisneri [8] for the LISA orbits and its response to GWs, and we consider the GWs emitted by circular, nonspinning binaries,

$$\begin{aligned} h_+(t) &= h(1+\cos^2\iota)\cos(2\pi f t+\varphi_0)\\ h_\times(t) &= -2h\cos\iota\sin(2\pi f t+\varphi_0), \end{aligned} \tag{46}$$

where ι is the inclination of the binary's orbital plane with respect to the line of sight to the solar-system barycentre (SSB), f is the frequency of the source as measured at the SSB, φ_0 is the initial phase and h is the overall GW strength.

The sensitivity to sinusoidal signals, for sources at a fixed position in the sky, has been defined traditionally as the GW strength h 'required to achieve a SNR of five in a one-year integration time, as a function of Fourier frequency' [19]. We follow [19] in computing not the sky-average of this position-wise sensitivity, but instead the GW strength h required to achieve an rms-averaged SNR of five for sources isotropically distributed over the sky. However, unlike [19], where polarization states are chosen uniformly over the abstract Poincaré sphere [20], we consider sources isotropically distributed over ι and over the GW polarization ψ (essentially a rotation of h_+ and $h_\times$ with respect to the principal axes conventionally defined at every sky position). In fact, we find empirically that the two distributions yield almost identical sky-averaged sensitivity curves.

The rms sky average has the advantage that the LISA orbital motion can be neglected, since the source distribution remains isotropic (and the sky-average invariant) as the LISA orientation changes along the year; thus, all SNRs can be computed for a stationary LISA sitting at the SSB. This approximation neglects the Doppler modulation of individual sources, which changes results only marginally by smoothing out the signals across nearby frequencies. Following [19], we can then operate in the frequency domain, as follows. For 10 000 uniformly sampled sky positions, inclinations and polarization states, we turn $h_+(t)$ and $h_\times(t)$ into complex phasors[5] that are inserted in the y_l GW responses (1)–(2) of [8], which in turn are inserted in the TDI expressions for the observables; delays are always replaced with Δ_l factors, and evaluated in the limit of equal armlengths. The squared modulus of the resulting phasor (which is a function of frequency through the Δ_l), multiplied by $T = 1$ year and divided by the noise PSD, yields the SNR^2, which can then be summed over noise-orthogonal observables and averaged over sky position, inclination and polarization.

Our results are shown in figure 2. As plotted in the bottom panel, the four-link configurations yield slightly different sensitivities depending on which type of observable can be constructed (X_i; U_i and V_i, which have the same sensitivity; or E_i and P_i, which also have the same sensitivity); however, they all converge in the low-frequency limit, and they essentially agree at high frequencies. The gain in upgrading to a five-link configuration is $\sqrt{2}$ in the low-frequency limit, and as much as $\sim\sqrt{3}$ at peak frequencies above 10 mHz. The further gain in upgrading from a four-link to a six-link configuration is again $\sqrt{2}$ in the low-frequency limit (because the third noise-orthogonal observable T is insensitive to GWs in that limit, as seen in the top panel), and as much as ~ 2 at peak frequencies above 10 mHz.

[5] With amplitudes reduced by $1/2$ to account for a constraint of reality on the GWs.

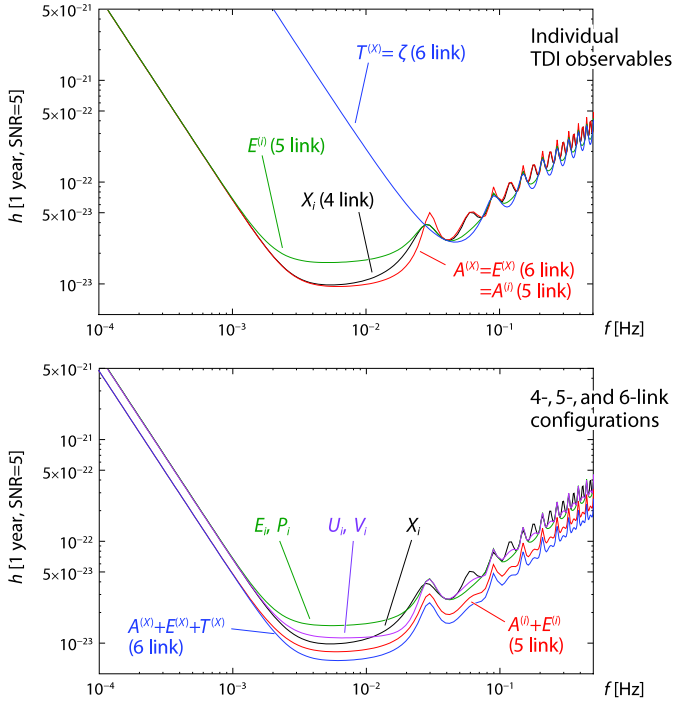

Figure 2. Bottom panel: LISA sensitivity to monochromatic sinusoidal signals in the six-link, five-link, and in all four-link configurations (which are different for X_i and for the two E_i/P_i and U_i/V_i pairs). Top panel: sensitivity of the individual noise-orthogonal observables in the six-link ($A^{(X)}$, $E^{(X)}$ and $T^{(X)}$) and five-link ($A^{(i)}$, $E^{(i)}$) configurations, as compared to the standard unequal-arm Michelson observable X_i.

7. Polarization-angle estimation error with four, five and six inter-spacecraft measurements

As a second example of the use of noise-orthogonal TDI bases to characterize the LISA performance under different failure scenarios, we now compute the expected estimation error for the GW polarization ψ of our fiducial monochromatic binaries, as predicted by the appropriate diagonal element of the inverse Fisher matrix (see, e.g., [21]). One of these binaries is completely described by seven parameters (ecliptic latitude and longitude, polarization, amplitude, inclination, frequency, and initial phase) so the full Fisher matrix that we invert is 7×7. To compute its elements, we work in the time domain with the full LISA GW response of [8] (including the amplitude and Doppler modulations due to the LISA orbital motion), and we compute signal derivatives with respect to source parameters by means of finite differences for very small parameter displacements. When more than one noise-orthogonal observable can be constructed, the corresponding Fisher matrices are summed before inverting to yield errors.

We consider 10 000 binary systems spread across the LISA band, with uniformly sampled sky positions, inclinations and polarizations; furthermore, we consider observations lasting one month, three months and one year, with four-link (X_1), five-link ($A^{(1)} + E^{(1)}$) and six-link ($A^{(X)} + E^{(X)} + T^{(X)}$) LISA configurations. Figure 3 shows the median polarization errors as a function of source frequency. The signal amplitudes were chosen individually for each

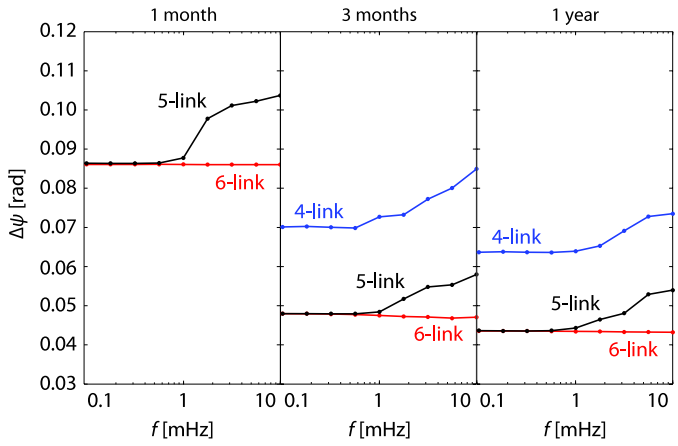

Figure 3. Median polarization uncertainty as a function of binary frequency, for 10 000 sources uniformly distributed over sky positions, inclinations and polarizations, as determined using four-, five- and six-link LISA configurations. The three panels show expected uncertainties for observations of 1 month, 3 months and 1 year. The signals are scaled so that their six-link SNR is 10; thus, the four- and five-link uncertainties are computed for signals that would have four- and five-link SNR less than 10.

system so that it would be detected with an SNR of ten by the full six-link LISA configuration, notwithstanding the observation timespan (thus, the one-year signals are intrinsically weaker than the three-month signals, and these in turn are weaker than the one-month signals). Several features in this figure are worth discussing:

- Errors improve in the longer observations, because the LISA orbits (which have a period of one year) can then modulate the LISA response more strongly, helping to disentangle the sky-position, polarization and inclination source parameters. This improvement is most noticeable between one-month and three-month observations, and especially so for the four-link configuration, for which the one-month errors are so large ($\simeq \pi/2$) that they are off the chart in this figure, and that polarization is essentially undetermined at SNR $= 10$ with four links.
- The five- and six-link errors coincide below 1 mHz, just as the five- and six-link SNRs do. Furthermore, above 1 mHz the ratio of the six-link to five-link errors agrees (within numerical noise) with the ratio of the six-link to five-link SNRs. Recalling that Fisher-matrix expected errors scale as SNR^{-1}, we see that the primary effect of switching from five- to six-link configurations is to improve estimation error by increasing the SNR, but not by providing complementary 'views' of the same signal with different geometries. (Thus, if the five-link curve is renormalized by setting the five-link SNR of all binaries to 10, it collapses onto the six-link curve.) Interestingly, the SNR-renormalized five- and six-link errors are almost constant between 0.1 and 10 mHz. This fact was already noticed by Crowder and Cornish [22]; unfortunately, explaining how it comes about requires delving into the analytic structure of the LISA response, and is beyond the scope of this paper.
- The four-link errors behave a bit differently: their ratio to the five- and six-link errors is also explained by the SNR^{-1} scaling, but only for observations of three months or longer. Below three months, the four-link errors get worse and worse (relative to the five- and six-link errors) as the observation time gets shorter. We observe this behaviour

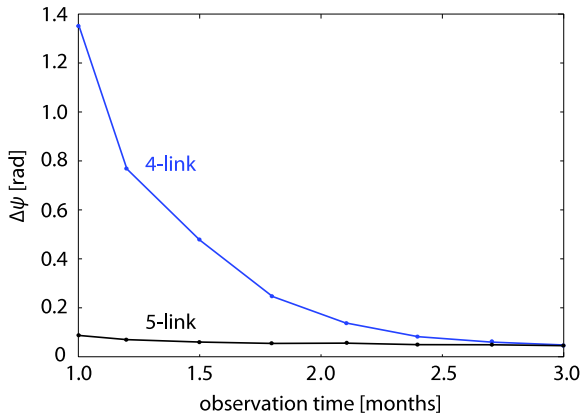

Figure 4. Median polarization uncertainty as a function of observation length, for 10 000 sources uniformly distributed over sky positions, inclinations and polarizations, as determined using four- and five-link LISA configurations. The signals are scaled separately before computing the four- and five-link errors so that their four- and five-link SNRs are both 10.

in figure 4, which plots the SNR-renormalized four- and five-link errors for binaries with GW frequencies between 1 and 1.1 mHz, as functions of observation time. The curves merge at three months, but the four-link errors degrade much more quickly than the five-link errors as observations get shorter. The apparent reason is that when we reduce the observation time, the polarization and sky-position parameters become more degenerate with four links than with five; correspondingly, the parameter errors become more correlated, and therefore individually larger. Thus the additional 'view' of the signal that is available with five links does help the polarization error, but only for rather short observations; above three months, its effect gets washed out by the greater amount of information provided by the longer orbital baseline.

8. Conclusion

We have discussed a simple framework to assess the LISA science performance (as indexed by its sensitivity to sinusoidal signals and by the inverse-Fisher-matrix parameter errors) in its full six-link configuration, and in failure modes where up to two inter-spacecraft laser measurements and up to four intra-spacecraft laser measurements become unavailable. We have described a unified, straightforward procedure to find the TDI observables that can be constructed in each failure mode, and to derive noise-orthonormal bases for them. In particular, we have given explicit expressions for the $A^{(i)}$ and $E^{(i)}$ orthonormal observables possible with five links, which had not previously appeared in the literature. Furthermore, we have demonstrated that both the SNR and the Fisher matrix are invariant under changes of TDI bases, so they depend only on which measurements are available, and can be computed for any convenient choice of observables. As an example of the application of our framework, we have computed the LISA sensitivity to sinusoidal signals in six-link, five-link and four-link configurations (figure 2) and the expected precision for the estimation of the polarization angle of monochromatic binaries in the three configurations (figure 3). The framework assumes a 'classic' conceptualization of the LISA noises and measurement, but we expect that our results could be adapted easily to the emerging 'strap-down' architecture without significant changes.

The framework can also be extended trivially to derivative LISA missions that include more than three spacecraft (such as the proposed 'bow-tie' LISA [23]) and possibly more than six inter-spacecraft measurements.

Acknowledgments

The authors are grateful to John Armstrong, Frank Estabrook, Tom Prince, Jan Harms, and to the anonymous referees for useful interactions. This work was carried out at the Jet Propulsion Laboratory, California Institute of Technology, under contract with the National Aeronautics and Space Administration. MV was supported by LISA Mission Science Office and by JPL's Human Resources Development Fund. MT was supported under research task 05-BEFS05-0014. The supercomputers used in this investigation were provided by funding from the JPL Office of the Chief Information Officer.

Appendix A. Multi-observable formulation of the noise inner product

The generalization of the standard noise inner product to multivariate processes (in this case, multiple TDI observables) follows from writing the probability of the stationary Gaussian vector process n_α as

$$p(\mathbf{n}) \propto \exp\left\{-\frac{1}{2}\int_{-\infty}^{+\infty} n_\alpha^*(f)\,{}^{(2)}S_{\alpha\beta}^{-1}(f)n_\beta(f)\,\mathrm{d}f\right\} \equiv \exp\{-(\mathbf{n},\mathbf{n})/2\}, \tag{A.1}$$

which is correct since the correlations are entirely described by the cross spectrum $\langle n_\alpha(f)n_\beta^*(f')\rangle = {}^{(2)}S_{\alpha\beta}(f)\delta(f-f')$. Using the fact that $S_{\alpha\beta}$ must be Hermitian, and furthermore that $S_{\alpha\beta}(-f) = S_{\alpha\beta}^*(f)$ (since $n(-f) = n^*(f)$ for real noise processes), and replacing ${}^{(2)}S_{\alpha\beta}(f)$ with the more familiar $S_{\alpha\beta} = 2\,{}^{(2)}S_{\alpha\beta}$ (which becomes the one-sided spectrum for $\alpha = \beta$), we can write

$$(\mathbf{g},\mathbf{h}) = 4\,\mathrm{Re}\int_0^{+\infty} g_\alpha^*(f)S_{\alpha\beta}^{-1}(f)h_\beta(f)\,\mathrm{d}f. \tag{A.2}$$

Note that the imaginary part of $S_{\alpha\beta}$ is crucial to computing this inner product correctly. $S_{\alpha\beta}$ can only be real if the correlation function $C_{\alpha\beta}(\tau) = \int_{-\infty}^{+\infty} n_\alpha(t+\tau)n_\beta(t)\,\mathrm{d}t$ is even, but this is never the case for TDI variables, which include time-delayed linear combinations of different noises. Consider for instance two noise processes $n_1(t)$ and $n_2(t) \equiv n_1(t-\Delta t)$:

$$C_{12}(\tau) = \int_{-\infty}^{+\infty} n_1(t+\tau)n_1(t-\Delta t)\,\mathrm{d}t = \int_{-\infty}^{+\infty} n_1(t+\tau+\Delta t)n_1(t)\,\mathrm{d}t = C_{11}(\tau+\Delta t). \tag{A.3}$$

Since for a stationary process n_1 the autocorrelation $C_{11}(\tau)$ is even, $C_{12}(\tau)$ cannot be even. It is true however that the imaginary part of $S_{\alpha\beta}$ may be disregarded in computing the cross power (i.e., integrating $S_{\alpha\beta}$ over all frequencies) for real processes, since then all imaginary contributions cancel between positive and negative frequencies.

Note that in this paper we adopt the Numerical Recipes [24] definition of the Fourier transforms, namely $h(f) = \int h(t)\exp^{2\pi\mathrm{i}ft}\,\mathrm{d}t$, $h(t) = \int h(f)\exp^{-2\pi\mathrm{i}ft}\,\mathrm{d}t$.

References

[1] Bender P and Danzmann P and the LISA Study Team 1998 *Laser Interferometer Space Antenna for the Detection of Gravitational Waves, Pre-Phase A Report MPQ No 233* (Garching: Max-Planck-Institüt für Quantenoptik)
[2] Tinto M and Dhurandhar S V 2005 *Living Rev. Rel.* **8** 4
[3] Estabrook F B, Tinto M and Armstrong J W 2000 *Phys. Rev.* D **62** 042002

[4] Cutler C 1998 *Phys. Rev.* D **57** 7089–102
[5] Tinto M 1998 *Phys. Rev.* D **58** 102001
[6] Tinto M, Estabrook F B and Armstrong J W 2002 *Phys. Rev.* D **65** 082003
[7] Tinto M, Armstrong J W and Estabrook F B 2008 *Class. Quantum Grav.* **25** 015008
[8] Vallisneri M 2005 *Phys. Rev.* D **71** 022001
[9] Vallisneri M 2005 *Phys. Rev.* D **72** 042003
[10] Cornish N J and Hellings R W 2003 *Class. Quantum Grav.* **20** 4851
[11] Tinto M, Estabrook F B and Armstrong J W 2004 *Phys. Rev.* D **69** 082001
[12] Schumaker B L 2007 Personal communication
[13] Golub G and van Loan C 1996 *Matrix Computations* 3rd edn (London: Johns Hopkins University Press)
[14] Romano J D and Woan G 2006 *Phys. Rev.* D **73** 102001
[15] Bodewig E 1959 *Matrix Calculus* (Amsterdam: North-Holland)
[16] Arnaud K A *et al* 2007 *Class. Quantum Grav.* **24** S551–64
[17] Prince T A, Tinto M, Larson S L and Armstrong J W 2002 *Phys. Rev.* D **66** 122002
[18] Nayak K R, Pai A, Dhurandhar S V and Vinet J-Y 2003 *Class. Quantum Grav.* **20** 1217–32
[19] Tinto M, Estabrook F B and Armstrong J W 2002 whitepaper on 'Time-Delay Interferometry and LISA's Sensitivity to Sinusoidal Gravitational Wave' available at www.srl.caltech.edu/lisa/mission_documents.html
[20] Huard S 1997 *Polarization of Light* (Chichester: Wiley)
[21] Vallisneri M 2008 *Phys. Rev.* D **77** 042001 (*Preprint* gr-qc/0703086)
[22] Crowder J and Cornish N J 2004 *Phys. Rev.* D **70** 082004
[23] Prince T A 2007 Personal communication
[24] Press W H, Flannery B P, Teukolsky S A and Vetterling W T 1988 *Numerical Recipes in C* (Cambridge: Cambridge University Press)